ISBN: 978-3-95450-184-7 doi:10.18429/JACoW-IPAC2018-TUPAK009

MUON PROFILE MEASUREMENT AFTER ACCELERATION WITH A RADIO-FREQUENCY QUADRUPOLE LINAC

M. Otani*, Y. Fukao, K. Futatsukawa, N. Kawamura, T. Mibe, Y. Miyake, K. Shimomura, T. Yamazaki, KEK, Oho, Tsukuba, 305-0801, Japan
Y. Sue, T. Iijima, Nagoya University, Nagoya, Aichi 464-8602, Japan
S Bae, H. Choi, S. Choi, B Kim, H. S. Ko, SNU, Seoul 08826, Republic of Korea
K. Hasegawa., Y. Kondo, T. Morishita, JAEA, Tokai, Ibaraki, 319-1195, Japan
H. Iinuma, Y. Nakazawa, Ibaraki University, Mito, Ibaraki 310-8512, Japan
K. Ishida, RIKEN, Hirosawa, Wako, 351-0198, Japan
R. Kitamura, S. Li, University of Tokyo, Hongo, Tokyo 171-8501, Japan
G. P. Razuvaev, BINP, SB RAS, Novosibirsk 630090, Russia
N. Saito, J-PARC Center, Tokai, Naka, Ibaraki 319-1195, Japan
E. Won, Korea University, Seoul 02841, Republic of Korea

Abstract

We have measured the muon beam profile after acceleration using a radio frequency quadrupole linac (RFQ). Positive muons are injected to an aluminum degrader and negative muoniums (Mu^-) are generated. The generated Mu^-'s are extracted by an electrostatic lens and accelerated to 89 keV by the RFQ. The accelerated Mu^-'s are transported to a beam profile monitor (BPM) through a quadrupole magnet pair and a bending magnet. The BPM consists of a micro-channel plate, a phosphor screen, and a CCD camera. The measured profile in the vertical direction is consistent with the simulation. This profile measurement is one of the milestones for realizing a muon linac for measurement of the muon anomalous magnetic moment at the Japan Proton Accelerator Research Complex.

INTRODUCTION

Though the discovery of the Higgs boson at the large hadron collider (LHC) completed the particles predicted in the Standard Model (SM) of elementary particle physics, some observations such as the existence of dark matter indicate new physics beyond the SM at some energy or interaction scale. One of the clues for new physics is the anomaly of the muon anomalous magnetic moment $(g-2)_\mu$; a difference of approximately three standard deviations exists between the SM prediction and the measured value (with a precision of 0.54 ppm) of $(g-2)_\mu$ [1]. Measurement with higher precision is necessary to confirm this anomaly. Low-emittance muon beams will facilitate more precise measurements, as the dominant systematic uncertainties in the previous experimental results are due to the muon beam dynamics in the muon storage ring.

The E34 experiment at the Japan Proton Accelerator Research Complex (J-PARC) [2] aims to measure $(g-2)_\mu$ with a precision of 0.1 ppm with a low-emittance muon beam. In the experiment, ultraslow muons with an extremely small transverse momentum of 3 keV/c (kinetic energy = 30 meV) are generated via thermal muonium production [3] followed by laser dissociation [4]. The generated ultraslow muons are electrostatically accelerated to 5.6 keV and injected into a muon linac. The muon linac consists of a radio frequency quadrupole linac (RFQ) [5], an inter-digital H-mode drift tube linac [6], a disk-and-washer coupled cell linac [7], and a disk loaded traveling wave structure [8]. In order to satisfy the experimental requirement of an extremely small transverse divergence angle of 10^{-5}, the muon should be accelerated to a momentum of 300 MeV/c without substantial emittance growth. Because the main reason for emittance growth in the muon linac is mismatch between the designed and actual beam ellipse in phase space, it is necessary to establish a beam diagnostic method.

Recently, we have succeeded in demonstrating muon acceleration using an RFQ [9]. In this experiment, negative muonium (Mu^-, $\mu^+ e^- e^-$) are generated from μ^+'s through the electron capture process in an aluminum degrader. The generated Mu^-'s are accelerated using the RFQ. Measurement of the Mu^- beam profile was conducted as part of the acceleration experiment. This paper describes the experimental setup, simulations, and results.

EXPERIMENTAL SETUP

Figure 1 shows the setup of the experiment. The J-PARC muon science facility (MUSE) [10] provides a pulsed surface muon (μ^+) beam with a 25-Hz repetition rate. The surface muons are decelerated by an aluminum degrader, and some portions form Mu^-'s. The Mu^-'s are extracted and accelerated to 5.6 keV by an electrostatic lens [11]. They are then injected to an RFQ. This RFQ was originally designed to accelerate negative hydrogen ions up to 0.8 MeV. In order to use this RFQ for muon acceleration, the inter-vane voltage is normalized to the mass ratio. The output energy in the case of moun is 89 keV. The accelerated Mu^-'s are detected by a beam profile monitor (BPM) after a diagnostic beamline. The diagnostic beamline consists of a magnetic quadrupole pair (QM1 and QM2) and a bending magnet.

* masashio@post.kek.jp

ISBN: 978-3-95450-184-7 doi:10.18429/JACoW-IPAC2018-TUPAK009

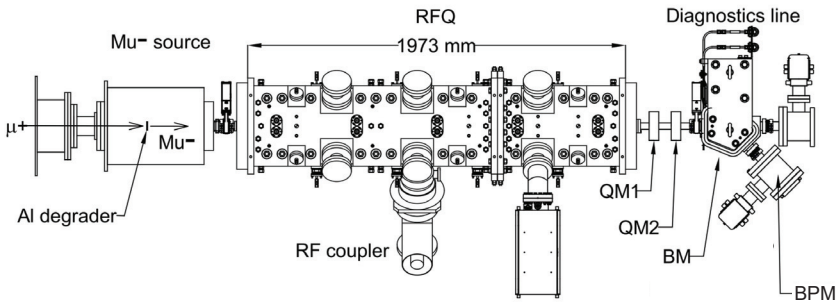

Figure 1: Schematic drawing of the experimental setup.

The diagnostic beamline was commissioned prior to the experiment using a H^- source: The H^-'s are generated by exposing an Al foil surface to ultraviolet light. The extracted kinetic energy of the H^-'s is set to 10 keV so that the momentum of the H^-'s is the same as that of the accelerated Mu^-'s. The field gradients of QM1 and QM2 were set to 2.6 T/m and 1.8 T/m, respectively, on the basis of the commissioning results and phase space distributions estimated by the simulations described in the next section.

Figure 2 shows a schematic view of the BPM, which consists of a micro-channel plate (MCP), a phosphor screen (P47), and a CCD camera. The MCP (Hamamatsu F2225-21P) has two stages of chevron-type MCPs with an effective area corresponding to a diameter of ϕ40 mm. The typical gain with a high-voltage setting during the experiment is 10^7. The P47 phosphor material is Y_2SiO_5 : Ce, and the decay time is 0.11 μs. The CCD camera (PCO pco.1600) with lens (Zeiss Distagon 2/28 ZF.2) collects light from the phosphor screen through a glass viewport. The BPM performance was evaluated using the surface muon beam at J-PARC prior to the experiment [12]. It was confirmed that the BPM has a sufficient spatial resolution of 0.3 mm and single muon counting performance.

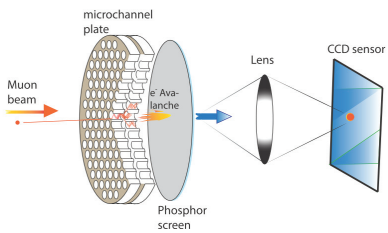

Figure 2: Schematic view of the beam profile monitor [12].

ADC data in all pixels (800 × 600 pixels with combined 2 × 2 binning mode) were taken with 500 ns exposure time in each 25-Hz beam pulse. The exposure time is set to the arrival time of the accelerated Mu^-'s. The arrival time was measured before data collection for profile measurement, and the obtained time is consistent with that of the previous experiment [9]. The main background in this experiment is decay positrons from muons; some of the incident muons penetrate the RFQ without acceleration and a decay positron accidentally goes to the MCP. In order to investigate the decay positron background, data with a 0.5 μs delay in arrival time was collected.

SIMULATIONS

The g4beamline simulation package [13] was used for simulation of the surface muon beamline to estimate the profile and intensity at the aluminum degrader. The estimated profile was verified by comparison with the measured beam profile at the focal point. The muon beam intensity is estimated to be 3×10^6/s, and 27% of the primary μ^+hit the aluminum degrader. The Mu^-phase spectra were implemented with proton data [14] scaled by velocity. Because little is known about the zero velocity region in [14], the yield was normalized by results from our prior experiment for the Mu^-measurement [15]. The conversion efficiency from positive muons to Mu^-'s with epi-thermal energy is on the order of 10^{-7}. The simulation of the electrostatic lens was performed using GEANT4 [16]. In the simulation, the electric field of the electrostatic lens is calculated by OPERA [17] and implemented. PARMTEQM [18] was employed for the RFQ simulation. For the end cell section, PIC simulation with GPT [19], in which the electric field was calculated with CST MW Studio [20], was employed to estimate the effects due to the unequal spacing of the vanes at the end. The transmission efficiency was estimated as 15%. Almost all the losses occurred in the RFQ entrance, because of much larger phase spaces than the RFQ acceptance. The transmission efficiency for the ultraslow muons is estimated to be more than 90%. TRACE3D [21] and PARMILA [22] were employed for the diagnostic beamline simulation. The transport efficiency is evaluated as 80%.

Figure 3 shows the calculated phase space distributions at the BPM location. The horizontal profile is wider than the vertical profile because of momentum dispersion. An chromatic beam transport system is being developed for the emittance measurement in the horizontal direction.

The simulation study about the alignment error was performed. The apparatuses in the diagnostic line were constructed with an accuracy of 0.2 mm. The beam emittance and the transport efficiency were not changed within several percent.

ISBN: 978-3-95450-184-7 doi:10.18429/JACoW-IPAC2018-TUPAK009

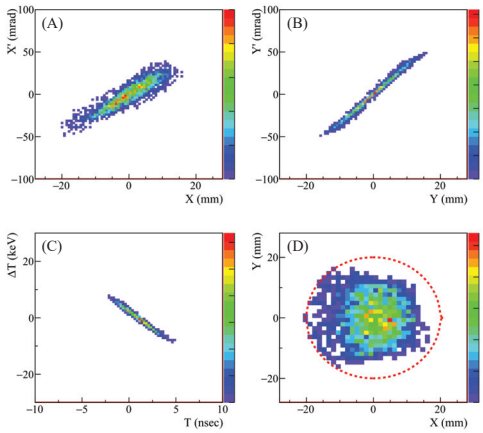

Figure 3: Calculated phase space distributions at the BPM location. (A) the horizontal divergence angle x' vs x, (B) the vertical divergence angle y' vs y, (C) $\Delta W(W-89\ \mathrm{keV})$ vs $\Delta\phi$, and (D) y vs x. The red dotted circle in (D) represents the BPM effective area.

ANALYSIS

The CCD pixel having the highest charge (Q_{peak}) in a picture is selected as an active pixel. An event cluster is defined as 9×9 pixels around the active pixel. In the event cluster, the total charge amount (Q_{total}) and the minimum and maximum root mean square in the cluster ($R_{\mathrm{min}}$and R_{max}) are calculated for further event selections. After the event cluster is eliminated, the next active pixel is searched in the picture. If Q_{total} is consistent with that from a CCD noise, the algorithm goes to the next picture.

The main background in this experiment is decay positrons from μ^+. Because almost all fractions of decay positrons are minimum ionization particles (MIPs), decay positrons can penetrate the MCP. In this case, the event shape is track-like, and R_{max} becomes large compared to a point-like event. Figure 4 shows the R_{max}distributions for two event samples: the red histogram is of the beam arrival timing, and the blue histogram is of the late timing. In the late timing, almost all the events are due to decay positrons. Under the R_{max} cut ($R_{\mathrm{max}} < 0.21$ mm), less than 10% of the events in the later timinig survived.

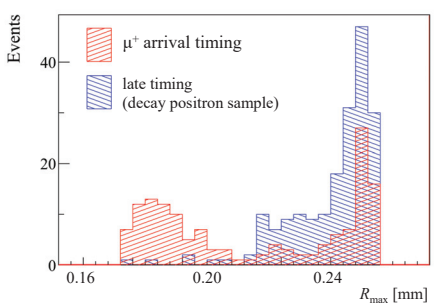

Figure 4: Distributions of root mean square in the major axis (R_{max}) for events of the muon arrival timing (red) and of the late timing (blue).

In addition to selection with R_{max}, charge information is used to eliminate decay positrons using the same method as in [9]; because the probability of generating secondary electrons in a decay positron event is lower than that of the accelerated Mu^-'s, the Q_{total} and Q_{peak} of decay positrons become smaller.

RESULTS

The measured profile was obtained after the event selections with R_{max}, Q_{total}, and Q_{peak} as described in previous section. The red histogram in Fig. 5 shows the horizontal and vertical profiles after the selections. The green histogram in Fig. 5 shows the expected profile obtained by the simulations. The Kolmogorov–Smirnov test was performed and the measurement and expectation were consistent within statistical error ($P = 21\%$ and $P = 33\%$ for the horizontal and vertical direction, respectively). The detailed simulations are being developed to improve the agreement between the measurement and simulation.

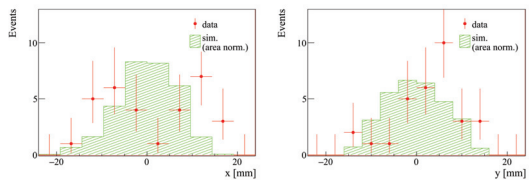

Figure 5: Red: measured beam profile in the horizontal direction (left) the vertical direction (right) after the event selections. Green: expected profile obtained by the simulations (projection to the x-axis in Fig. 3 (A) and (B), respectively. .

This profile measurement is a critical step toward establishing a diagnostic method in the muon linac. Further investigations such as emittance measurement by scanning the quadrupole strength can be performed with a higher beam intensity. The new muon beamline being assembled in J-PARC MUSE will provide approximately eleven times larger incident muon flux. There is also the possibility of improving the $\mu^+ \rightarrow \mathrm{Mu}^-$conversion efficiency by cesiation as with H^- ion sources [23]. Finally, the laser-dissociation ultraslow muon source is expected to be installed in the new beamline to obtain a muon rate of 10^6/s.

SUMMARY

In summary, the muon beam profile was measured after acceleration using the RFQ. Slow Mu^-were generated by injecting μ^+'s to the degrader and accelerated with the RFQ up to 89 keV. The accelerated Mu^-'s were transported to the BPM through the quadrupole magnet pair and the bending magnet. The measured beam profile was consistent with the simulations within statistical error. This measurement is one of the milestones for establishing a beam diagnostic method in the muon linac for the J-PARC muon g-2 experiment.

ISBN: 978-3-95450-184-7 doi:10.18429/JACoW-IPAC2018-TUPAK009

ACKNOWLEDGMENT

This work is supported by JSPS KAKENHI Grant Numbers JP25800164, JP15H03666, JP18H03707 , JP16H03987, JP15H05742, and JP16J07784. This work is also supported by the Korean National Research Foundation grants NRF-2015H1A2A1030275, NRF-2015K2A2A4000092, and NRF-2017R1A2B3007018; and the Russian Foundation for Basic Research grant RFBR 17-52-50064; This experiment at the Materials and Life Science Experimental Facility of the J-PARC was performed under user programs (Proposal No. 2017B0006).

REFERENCES

[1] G.W. Bennett *et al.*, *Phys. Rev.* D **73**, 072003, 2006.

[2] http://g-2.kek.jp/portal/index.html

[3] G.A. Beer *et al.*, Prog. Theor. Exp. Phys. **091**, C01, 2014.

[4] P. Bakule *et al.*, Nucl. Instru. Meth. B **266**, 335, 2008.

[5] Y. Kondo *et al.*, "Simulation Study of Muon Acceleration Using RFQ for a New Muon G-2 Experiment at J-Parc", in Proceedings of IPAC2015 (Richmond, VA, USA, 2015), pp. 3801–3803.

[6] M. Otani *et al.*, *Phys. Rev. Accel. Beams* **19** 040101 (2016).

[7] M. Otani *et al.*, "Development of Muon Linac for the Muon G-2/EDM Experiment at J-Parc", in Proceedings of IPAC2016 (Busan, Korea, 2016), pp. 1543–1546.

[8] Y. Kondo *et al.*, Journal of Physics: Conference Series **874**, 012054 (2017).

[9] S. Bae *et al.*, 2018 *Preprint* arXiv:1803.07891 [physics.acc-ph]

[10] Y. Miyake *et al.*, Journal of Physics: Conference Series **225**, 012036 (2010).

[11] K. F. Canter *et al.*, in "Positron studies of solids, surfaces and atom" (World Scientific, Singapore, 1986) p. 199.

[12] B. Kim *et al.*, submitted to Nucl. Instru. Meth. A

[13] G4beamline, http://public.muonsinc.com/Projects/G4beamline.aspx

[14] M. Gonin *et al.*, Rev. of Sci. Instr. **65**, 648 (1994).

[15] R. Kitamura *et al.*, Journal of Physics: Conference Series **874**, 012055 (2017).

[16] Geant4, http://geant4.cern.ch/

[17] OPERA3D, Vector Fields Limited, Oxford, England., https://operafea.com/

[18] K. R. Crandall *et al.*, "RFQ Design Codes," LA-UR-96-1836 (1996).

[19] General Particle Tracer, Pulsar Physics. [http://www.pulsar.nl/gpt/]

[20] CST Studio Suite, Computer Simulation Technology (CST). [https://www.cst.com/products/CSTMWS]

[21] K.R. Crandall and D.P. Rustoi, Los Alamos Report, No. LA-UR-97-886, 1997.

[22] Los Alamos Accelerator Code Group (LAACG), LANL, Los Alamos, [http://www.laacg.lanl.gov].

[23] V. Dudnikov *et al.*, "Cold Muonium Negative Ion Production", in Proceedings of IPAC2017 (Copenhagen, Denmark, 2017), pp. 2898–2901. https://doi.org/10.18429/JACoW-IPAC2017-WEPAB137 .